

# Scaling Ergodic Control for Large-Scale Problems: Robotic Exploration with a Moving Gaussian Mixture Model

Adam Seewald<sup>1</sup>, Ian Abraham<sup>2</sup>, and Stefano Mintchev<sup>1</sup>

**Abstract**—The problem of exploring unknown and large-scale spaces with robots arises in many real-world applications. While different approaches exist, those utilizing sensory data have emerged as of particular interest. Among these, ergodic control is significant, as it accounts for both motion cost and optimality. However, ergodic controllers often encounter limitations when applied to large-scale problems. This paper introduces a general and scaled ergodic control methodology designed to overcome these limitations. Unlike traditional ergodic controllers that rely on predefined information measures or separate obstacle avoidance, our approach dynamically generates and refines the information measure from sensory data and derives a degree of obstacle avoidance as a “by-product.” Empirical data from simulations in diverse environments, including dense vegetation and agricultural settings, demonstrate the effectiveness of our scaled general ergodic control, showcasing the applicability of our methodology compared to conventional techniques typically restricted to structured or small-scale only.

## I. INTRODUCTION

Exploring unknown and potentially large-scale spaces with robots is a problem commonly addressed by different methodologies arising in computing and robotics. This problem is recurring in real-world use cases such as monitoring, reconstruction, exploration, etc., where robots are expected to cover a given space while performing an assigned task. A key challenge to the practical applicability of these methodologies is that of leveraging resources while, at the same time, maximizing the information gathered and optimizing the exploration accordingly [1, 2]. While there are different approaches in the literature, approaches that are informed by sensory data have emerged as of particular interest. Among these approaches, ergodic control is a significant result, as it provides a more natural way of searching through deterministic exploratory behaviors while accounting for both the motion cost and optimality [3].

Ergodic control is a planning and controls methodology that derives robot trajectories maximizing a given information measure so that robots spend more time in areas with high information measure while quickly traversing areas with low information measure [4–6]. As a consequence, it is required that the user provides an information measure a priori or that the information measure is derived as the robots gather more information about their surroundings. While applicable to some use cases, this is often a limitation of the existing

This work was partly supported by ETH Zürich’s World Food System Center and Yale University.

<sup>1</sup>A.S. and S.M. are with the Department of Environmental Systems Science, ETH Zürich, Switzerland. Email: [aseewald@ethz.ch](mailto:aseewald@ethz.ch);

<sup>2</sup>I.A. is with the Department of Mechanical Engineering and Materials Science, Yale University, CT, USA.

ergodic controllers. It is not always the case that the information measure can be easily refined from the gathered data, or that an a priori information measure can be provided at all. Furthermore, it is also not always feasible to define an information measure for large-scale spaces in practice. With this work, we address this challenge. We provide a general and scaled ergodic control methodology that can be applied to a broader class of robotic use cases. Our methodology does not require an underlying information measure but rather, derives an information measure from the exploration itself and refines such a measure utilizing information about already visited areas and obstacles from sensory data. In contrast to existing ergodic control methodologies that require external obstacle avoidance techniques, e.g., control barrier functions [7], optical flow [8], etc., our methodology provides additionally a tunable degree of obstacle avoidance as a “by-product.” The underlying information measure is represented utilizing a Gaussian Mixture Model (GMM), which is refined from the sensory data as the robot traverses the state space – a process that is handled by our methodology and that does not require any user input. Our ergodic formulation is different from existing methods. The problem is posed so that the robot spends time in areas with low information measures, whereas the “explored space” is related to high information measures. The methodology is iterative and utilizes a model predictive controller (MPC) approach, where the ergodic controller is refined within a specified time window.

Existing ergodic controllers have been studied from the point of view of time [9] and energy [10, 11] optimality and applied to a multitude of use cases. These use cases include tactile sensing [5], active learning [12], multi-objective optimality [13, 14], grasping and manipulation [15, 16], and visual rendering [17, 18]. Ergodic controllers in the literature feature diverse aspects such as stochastic dynamics [19, 20] and multi-agent and/or swarm control with both centralized [10, 21] and distributed information processing [8, 22]. Although some of these use cases involve information gathering [23] and feature urban environments and other potentially large-scale problems [8, 24], a generic large-scale ergodic controller has not been studied yet. Even though recent methods have been making progress in this direction [9–11, 25], these methods do not scale efficiently due to the formulation of the underlying optimization and/or require an a priori information measure. From an obstacle avoidance perspective, even though there are ergodic controllers that feature obstacle avoidance [7], this is an external component on top of the ergodic controller that then results in a sub-ergodic solution [9] rather than an integral component of the

explorer itself.

We showcase our general and scaled ergodic control on a large-scale problem: the problem of exploring a simulated forest and an outdoor area that has both dense vegetation and an agricultural setting, in contrast to existing ergodic control methodologies that are demonstrated in structured environments or generally in small-scale only. Section IV shows the performance of our methods. The open-source software stack to replicate our approach and the experimental data are made available on our project repository webpage<sup>1</sup>.

The remainder of this paper is structured as follows. Sec. II provides the details of the underlying principles and the problem addressed. Sec. III is split into two sub-sections: one provides an overview of ergodic control, whereas the other details our methodology. Sec. V provides conclusions and draws future perspectives.

## II. PROBLEM FORMULATION

This work addresses the problem of exploring a bounded and potentially large-scale space, where “large-scale” refers to spaces on the order of dozens or even hundreds of meters in both the x- and y-axes. For practical reasons, we restrict the exploration space to one hectare and consider exploration in two dimensions. However, the formulation is such that the state space could potentially be unbounded and not limited to two dimensions [9].

Let us consider a bounded space  $\mathcal{Q} \subset \mathbb{R}^2$ . The robot is free to move in this space except for a finite number of obstacles represented by  $\mathcal{O} \subset \mathcal{Q}$ . In the remainder, we utilize the concepts of ergodicity and ergodic metric to direct the robot into unexplored areas (i.e., with low information density) while avoiding the obstacles, i.e.,  $\mathcal{Q} \cap \mathcal{O}$ , as opposed to other literature on ergodic control in the literature where exploration happens in areas of high information density instead [4–6].

**Definition II.1** (Ergodicity). Given the bounded state space  $\mathcal{Q}$ , a trajectory  $\mathbf{x}(t) \in \mathcal{Q}$  is *ergodic* with respect to a spatial distribution  $\phi$ , or, analogously, is distributed among regions of high expected distribution, if and only if

$$\lim_{t \rightarrow \infty} \int_{\mathcal{Q}} \phi(\mathbf{x}) \Omega(\mathbf{x}) d\mathbf{x} = \frac{1}{t} \int_{\mathcal{T}} \Omega(\bar{\mathbf{x}}(t)) dt, \quad (1)$$

where  $\bar{\cdot}$  is a map that maps the state space to the exploration spaces, and  $\Omega$  are all the Lebesgue functions as defined in, e.g., [4].

The spatial distribution  $\phi$  is constructed using a Gaussian Mixture Model (GMM).

**Definition II.2** (Moving GMM). Assume that there is a given number  $n \in \mathbb{N}_{>0}$  of Gaussians  $\mathcal{N}$  in a GMM, with an initial probability equally distributed. A *moving GMM* is

$$\phi(\boldsymbol{\alpha}, \boldsymbol{\mu}, \mathbf{x}) := \sum_{i=1}^n \alpha_i \mathcal{N}_i(\mathbf{x} | \mu_i, \Sigma_i), \quad (2)$$

where  $\Sigma_i \in \mathbb{R}^{2 \times 2}$  indicates the covariance matrix and  $\mu_i \in \mathcal{Q}$  denotes the center of a Gaussian  $\mathcal{N}_i$ . The GMM also has

variable centers  $\boldsymbol{\mu} \in \mathcal{Q}^n$  and variable mixing coefficients  $\boldsymbol{\alpha} \in \mathbb{R}_{>0}^n$ .

The notation  $\mathbb{S}_{>0}$  denotes a strictly positive set  $\mathbb{S}$ . Bold letters indicate vectors, i.e.,  $\mathbf{x} \in \mathcal{Q}$  is the state space vector, whereas  $\boldsymbol{\alpha}$ ,  $\boldsymbol{\mu}$  are the vectors comprising the ideal GMM’s mixing coefficients and position components respectively (see Sec. III).

An ergodic metric is then defined as a value that quantifies the ergodicity.

**Definition II.3** (Ergodic metric). Consider a time average distribution of the trajectory over a limited time window  $t$ , e.g.,

$$h(\mathbf{x}(t)) := \frac{1}{t} \int_{\mathcal{T}} \Delta((\mathbf{x})(t)) dt, \quad (3)$$

where  $\Delta$  is defined as a Dirac delta function. An *ergodic metric* is an  $L^2$ -inner product in between the average of the spatial and time distributions.

**Problem II.1** (Scaled ergodic control). Given the state space and the obstacles space  $\mathcal{Q}$  and  $\mathcal{O}$  respectively, assume the number of Gaussian components  $n$  is given. The *scaled ergodic control* problem is the problem of finding the evolution of the Gaussian components of a moving GMM, i.e.,  $\boldsymbol{\alpha}(t)$  and  $\boldsymbol{\mu}(t)$  and of the control  $\mathbf{u}(t) \in \mathcal{U}$  so that  $\mathbf{x}(t)$  explores  $\mathcal{Q}$  while avoiding  $\mathcal{O}$  and the ergodic metric is minimized.

We note that it is not a requirement that the obstacle space  $\mathcal{O}$  is known at the beginning of the exploration.

We propose a solution to Problem II.1 and demonstrate experimentally the feasibility of the solution, highlighting the trade-offs between accuracy (i.e., coverage) and exploration soundness (i.e., obstacle avoidance capabilities) in Sec. IV-A and IV-B respectively.

## III. METHODS

This section details our methods. Sec. III-A introduces the concept of canonical ergodic control for exploration in bounded areas with an information density distribution. Sec. III-B describes our methodology of scaled ergodic control, i.e., ergodic control with a moving information density as a function of explored versus unexplored space.

### A. Canonical ergodic control

To quantify the time average and the average of the spatial distributions  $h$  and  $\phi$  respectively, we use Fourier series basis functions, a common method for evaluating distributions in the spectral domain [4]. For the time average distribution, the coefficients of an equivalent basis function can be expressed as

$$c_k(\mathbf{x}(t)) := \int_{\mathcal{T}} \prod_{d \in \{1, 2\}} \cos(2\pi k_d \mathbf{x}_d(\tau)/T) / T^2 d\tau / t, \quad (4)$$

where  $T \in \mathbb{R}_{>0}$  is a given period and  $\cdot_d$  denotes the  $d$ th item of a vector.

Equation (4) expresses the cosine basis function for a coefficient  $k$ , considering only the positive slice of the spectral domain and thus ignoring the function’s imaginary

<sup>1</sup>[github.com/adamseew/scaledergo](https://github.com/adamseew/scaledergo)

component. The coefficients  $k \in \mathcal{K}$  depend on a given number of frequencies  $\kappa \in \mathbb{N}_{>0}$ , including the base frequency, and are constructed so that  $\mathcal{K} \in \mathbb{N}^2$  is a set of index vectors covering the set  $\kappa \times \dots \times \kappa \in \mathbb{N}^{\kappa^2}$ , i.e., they are built so that the coefficients are evaluated over the entire domain [26].

For the average of the spatial distribution, the coefficients of an equivalent basis function can be expressed similarly as

$$\phi_k(\mathbf{x}) := \int_{\mathcal{Q}} \sum_{d \in \{1,2\}} \phi(\mathbf{x}) c(\mathbf{x}) d\mathbf{x}, \quad (5)$$

where  $c$  is the integrand in Eq. (4) at the given point  $\mathbf{x}$ , evaluated at the current time step.

The aim of an ergodic controller is to minimize an ergodic metric, i.e., the  $L^2$ -inner product of the distributions  $h$  and  $\phi$  (see Definition II.3). A consolidated metric [5, 7, 9, 10, 12, 27] for this purpose is, for instance,

$$\mathcal{E}(\mathbf{x}) := \sum_{k \in \mathcal{K}} \Lambda_k (c_k - \phi_k)^2 / 2, \quad (6)$$

where the coefficients of the time average and the average spatial distributions are expressed in Eq. (4–5).

$\Lambda_k$  is a weight factor that determines the importance of different frequencies, e.g., with

$$\Lambda_k := \frac{1}{\sqrt{(1 + \|k\|^2)^3}}, \quad (7)$$

lower frequencies are preferred.

Note that in Eq. (5) we have utilized the expression for a standard GMM. We use the expression for the moving GMM defined in Definition II.2 (i.e., GMM with variable centers and mixing coefficients) in the next section.

### B. Scaled ergodic control

To utilize the concept of moving information density as a function of explored against unexplored space, let us first consider Eq. (5) with the moving GMM.

Let us assume for practical purposes that the space is square, with a given length  $l \in \mathbb{R}_{>0}$  expressed in meters. Let us thus tight the period in Eq. (4) to such search space and express  $l = T/2$ . Eq. (5) can be then also expressed

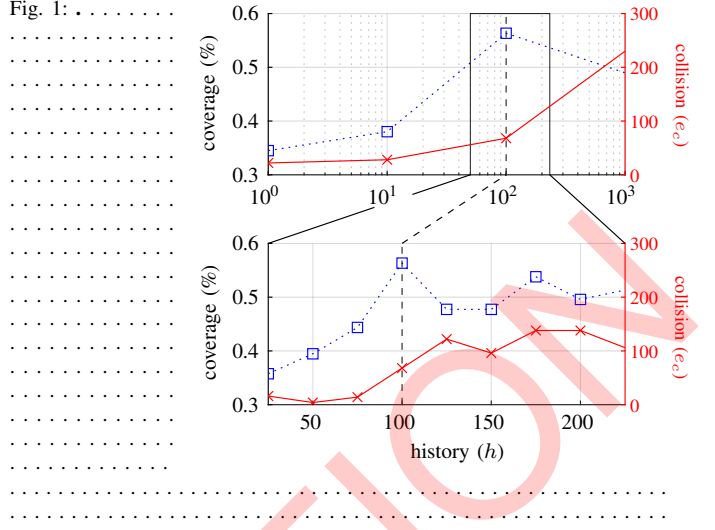
$$\phi_k(\boldsymbol{\alpha}, \boldsymbol{\mu}, \mathbf{x}) := \int_{\mathcal{Q}} \left( \sum_{d \in \{1,2\}} \sum_{i=1}^n \alpha_i \mathcal{N}_i(\mathbf{x} | \bar{\mu}_i, \bar{\Sigma}_i) \right) c(\mathbf{x}) d\mathbf{x}, \quad (8)$$

where  $\bar{\cdot}$  is a map that maps the center and the covariance matrix to a symmetric state space delimited by  $-l$  and  $l$  by, e.g., using linear transformation matrices [26].

Let us further define a given value that expresses the concept of ‘‘history.’’ If this value is expressed by,  $h \in \mathbb{R}_{>0}$ , we can model the space that has been already explored by the robot exploiting the definition of the moving GMM. The covariance matrix can be expressed

$$\Sigma_i := \frac{1}{2T} \int_{\Upsilon} \sum_{d \in \{1,2\}} (\mathbf{x}_d(\tau) - \mu_i) d\tau, \quad (9)$$

where the trajectory is being evaluated within the history, i.e.,  $\Upsilon$  indicates the time interval in between  $t$  and  $t - h$ .



The centers can be then expressed as  $\mu_i := E(\mathbf{x}(t))$  with  $E$  being the expected value of  $\mathbf{x}$  on  $\Upsilon$ .

The scaled ergodic control problem can then be expressed as the problem of finding an ergodic controller that visit the inverse of the probability distribution represented by the moving GMM, thus avoiding areas ‘‘already visited,’’ within a given history window  $h$ . The problem posed in this way, however, produces trajectories that require an additional obstacle avoidance methodology, such as [7].

Let us thus consider a modified expression for the center of the gaussian  $\mu_i := E(\mathbf{x}(t)) - e_i$  where  $e_i \in \mathbf{e} \subset \mathbb{R}^n$  is a displacement that allow to ‘‘move’’ the Gaussian components in the moving GMM.

Our methodology is such that the scaled ergodic controller finds the minimum displacement of the Gaussians so that the the space to be visited is delimited by  $\mathcal{Q} \cap \mathcal{O}$ . Such controller can be expressed with the optimal control problem (OCP)

$$\min_{\Theta} \mathcal{E}(\mathbf{x}) + \Psi(\mathbf{e}), \quad (10a)$$

$$\text{s.t. } \dot{\mathbf{x}} = f(\mathbf{x}(t), \mathbf{u}(t)), \quad (10b)$$

$$\mathbf{x}(t) \in \mathcal{Q} \cap \mathcal{O}, \mathbf{u}(t) \in \mathcal{U}, \quad (10c)$$

$$\mathbf{x}(t_0), n, \kappa, l, h, \text{ are given,} \quad (10d)$$

where the output of the optimization  $\Theta$  in Eq. (10a) is  $\mathbf{x}, \mathbf{u}, \boldsymbol{\alpha}, \boldsymbol{\mu}$ , i.e., the center of each Gaussian and its mixing coefficient in the moving GMM along the control and the state. The function  $\Psi$  maps the displacement to a cost value, e.g.,  $\Sigma_{e_i \in \mathbf{e}} |e_i|$ , where  $|\cdot|$  is the defined as an  $L^2$ -norm.

The dynamics in Eq. (10b) is a 2D single integrator system, which mimics the behaviour of an unmanned aerial vehicle (UAV) in our experimental setup to a reasonable extent (see Sec. IV).

The problem is formulated so that it finds displacement, and probability for each Gaussian and the optimal (i.e., ergodic) control, ensuring that the displacement and probability deviate minimally from the ideal case. Note once again that here the Gaussians represent the history of the explored space. For practical purposes, a given horizon  $N \in \mathbb{N}_{>0}$  is defined, and the optimization is reiterated for each horizon

using a methodology similar to an MPC controller, i.e.,  $\mathcal{T}$  in Eq. (4) is the interval in between  $t$  and  $t - N$  ( $N$  is not to be confused with the history window  $h$ ).

The large-scale exploration is considered concluded when a desired level of coverage is achieved (see Sec. IV). It is also possible to set up the problem so that the exploration does not terminate or lasts for long-term, such as in [28].

Other practical considerations, such as the choice of the history and the size of the moving GMM, are detailed in the next section.

#### IV. EXPERIMENTAL RESULTS

This section provides an overview of our experimental setup and showcases the results. Experiments are implemented utilizing MATLAB (R), whereas interfaces for physical experimental evaluation are aided by a routine implemented in Python. The MPC optimization stack, i.e., the solver that solves the OCP in Eq. (10), relies on two external open-source components. The non-linear programming solver IPOPT [29] and the algorithmic differentiation library CasADi [30].

In the following, Sec. IV-A describes experimental results, a simulated forest with an area of 3 600 squared meters. Sec. IV-B details our finding in terms of built-in obstacle avoidance capabilities against coverage of our general scaled ergodic controller. Sec. IV-C describes our outdoor modeled results, consisting of an area with both dense vegetation and an agricultural setting, compromising multiple obstacles and a total area of 10 000 squared meters.

##### A. Simulated forest

Simulated results are conducted in a forest with 45 trees spread randomly in area of 3 600 squared meters. The history  $h$  is set to 100 time steps (see Sec. IV-B). The simulation is terminated at 50 000 time step, when a desired coverage threshold is achieved within a certain approximation (i.e., 60%  $\pm$  5%). The number of Gaussians  $n$  is set to five, whereas the initial position is set to the middle of the state space. The number of frequencies  $\kappa$  is set to nine, excluding the base frequency, which in line with other ergodic controllers in the literature [28].

Fig. 2 shows the results for the simulated forest at three distinct time steps. Fig. 2a shows the trajectory (right of the figure) after 1 000 time steps. The history is illustrated with the dark-red line and the current point with the dark-red dot. The top-left of the figure shows the underlying information density distribution (i.e., the moving GMM in Definition II.2) with a detail of the five Gaussian components in the area that represents the current history interval. The optimal value of the Gaussians centers  $\mu$  and of the mixing coefficients  $\alpha$  are such that the moving GMM represents the history (i.e., the expected value and the covariance of the trajectory on the current history window) and that the Gaussians are deviated as little as possible to avoid the obstacles. The bottom-left of the figure shows the coverage map, where each square counts the number of points in within the square in a given time.

Fig. 2b shows the trajectory at time instant 2 500. The simulated UAV keeps flying through the obstacles, exploring

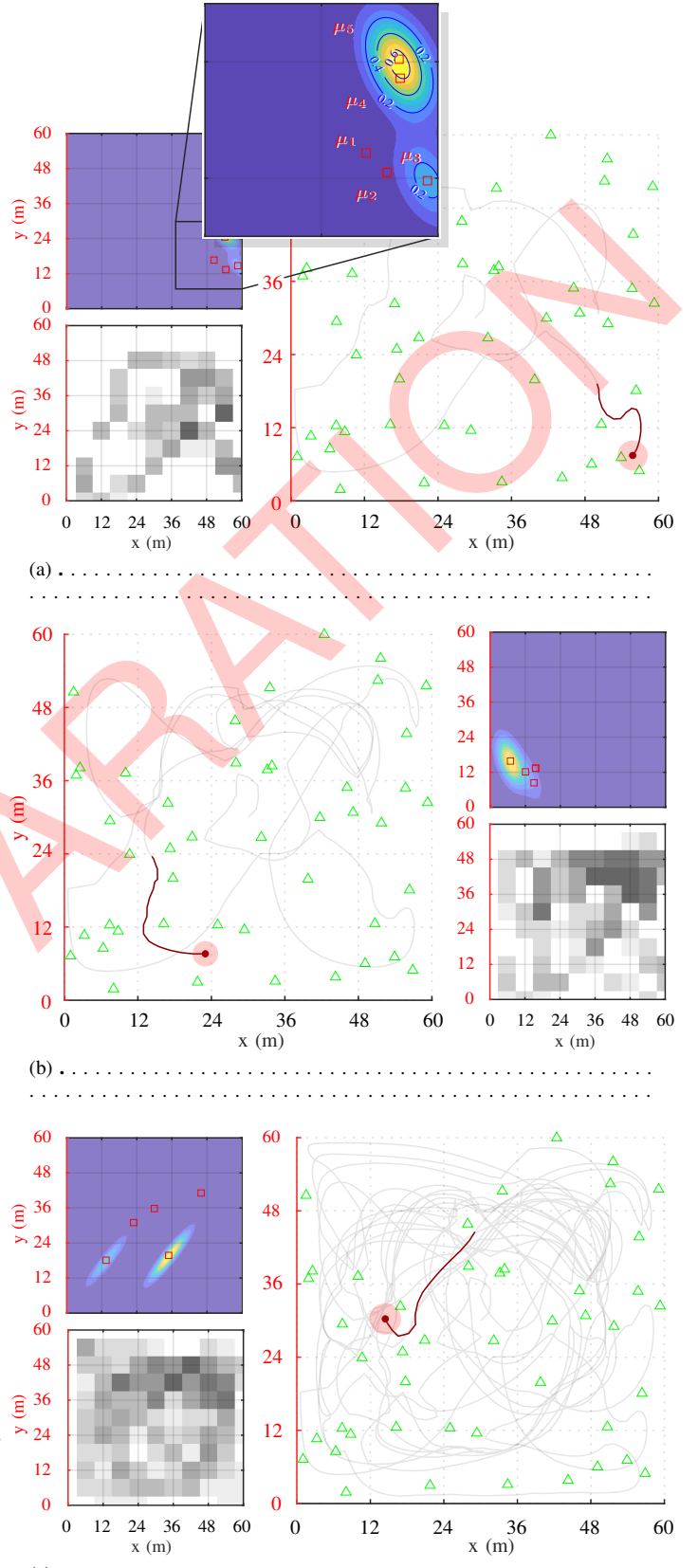


Fig. 2:

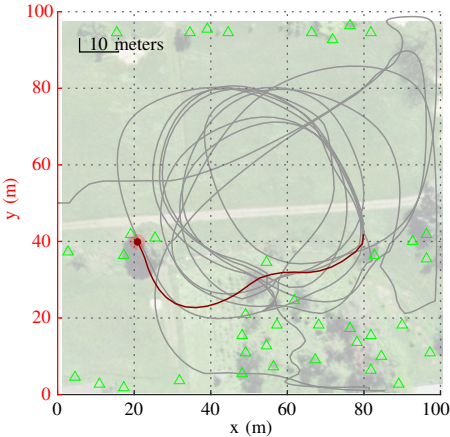


Fig. 3: . . . . .  
the shows a detail of the history window around 100, +/- 25.

### C. Outdoors model

Additional experimental evaluation is derived utilizing a model of an outdoors vegetated area situated in Birmensdorf ZH, Switzerland. The origin is set to 47.362646, 8.457228 in longitude and latitude coordinates. The area has been chosen so that it contains both dense vegetation and an agricultural setting, which mimics a potential real-world use case for our general scaled ergodic controller. The overall area being explored is bounded to 10 000 square meters and its surrounding has been surveyed manually to explore potential future feasibility.

Fig. 3 reports the path whereas the history is illustrated with the dark-red line and the current point with the dark-red dot. The history is set to 150 time steps and the dynamics in Eq. (10b) is adjusted so that the model mimics the UAV, a DJI Mavic 3 reasonably. The history is chosen so that the obstacles are avoided, i.e., the UAV avoids the trunks even though it is still able to fly in-within the vegetation. The physical experimental evaluation has been conducted on just an initial slice of the overall trajectory, demonstrating the eventual feasibility of the method in terms of utilizing ergodic controllers but the actual path is derived MATLAB (R). Further physical evaluation is currently being evaluated (see Sec. V). The exploratory trajectories are imported into the UAV's flight controller utilizing waypoints, which is handled by a proprietary software component; but portability with other software components and flight controllers is supported. The data are reported after a horizon of 5 000 time steps. The obstacles are placed so that the UAV travels in within the canopy, at an altitude of 2.5 meters. Which means that small bushes are not counted whereas tree trunks are. The velocity is set to 1.5 meters per second.

further the state space. The moving GMM is then shown on the top-right, whereas the coverage map is shown at the bottom-right.

Fig. 2c shows the trajectory at time instant 10 000. Similarly to the previous figures, the moving GMM model and the coverage are illustrated at the top-left and bottom-left respectively. One can notice that while the obstacles are overall avoided, the simulated UAV come close or even passes through the obstacles at times. We report a relation in between the degree of obstacle avoidance capabilities and the coverage, as discussed in the next section.

#### B. Obstacle avoidance vs. coverage

The OCP posed as Eq. (10) have no optimal solution. In this scenario, our algorithm is such that a sub-optimal solution is returned, where the constraint expressed in Eq. (10c) is not respected, e.g., the simulated trees in Sec. IV-A are not avoided with the desired threshold. While we found this behavior happening in an initial iteration of our scaled ergodic methodology, we have noticed that we can tune have well we can avoid the obstacles as a by-product of our approach utilizing the concept of history  $h$ .

Fig. 1 reports our experimental results in terms of built-in obstacle avoidance capabilities against coverage and a collision metric, underlying the trade-offs in between these metrics. The collision metric  $e_c$  is built so that every occurrence of a point that invalidates the constraint in Equation (10c) within a given threshold is counted. The actual count of occurrences is then reported on the left y-axis of the figure, with the horizon being set to 50 000, i.e., the actual invalidation ratio for a history window set to zero is solely 0.044 %, whereas is up an order of magnitude higher for a history window set to 1 000 (0.46 %). In all the experiments, the threshold is set to 60 centimeters. The coverage is calculated in the same way as reported in Sec. IV-A. It is to be noted that full coverage is not achieved, as obstacles are also counted in the overall coverage metric.

The top of the figure reports the three metrics on a logarithmic scale. Here we have noticed that a history window set to 100 provides the best trade-off in terms of obstacle avoidance

## V. CONCLUSION AND FUTURE DIRECTIONS

## REFERENCES

- [1] M. Popović, T. Vidal-Calleja, G. Hitz, J. J. Chung *et al.*, “An informative path planning framework for UAV-based terrain monitoring,” *Autonomous Robots*, vol. 44, no. 6, pp. 889–911, 2020. 1
- [2] L. Schmid, M. Pantic, R. Khanna, L. Ott *et al.*, “An efficient sampling-based method for online informative path planning in unknown environments,” *IEEE Robotics and Automation Letters*, vol. 5, no. 2, pp. 1500–1507, 2020. 1
- [3] L. M. Miller, Y. Silverman, M. A. MacIver, and T. D. Murphey, “Ergodic exploration of distributed information,” *IEEE Transactions on Robotics*, vol. 32, no. 1, pp. 36–52, 2016. 1
- [4] G. Mathew and I. Mezić, “Metrics for ergodicity and design of ergodic dynamics for multi-agent systems,” *Physica D: Nonlinear Phenomena*, vol. 240, no. 4, pp. 432–442, 2011. 1, 2
- [5] I. Abraham, A. Prabhakar, M. J. Z. Hartmann, and T. D. Murphey, “Ergodic exploration using binary sensing for nonparametric shape estimation,” *IEEE Robotics and Automation Letters*, vol. 2, no. 2, pp. 827–834, 2017. 1, 2, 3
- [6] L. M. Miller and T. D. Murphey, “Trajectory optimization for continuous ergodic exploration,” in *IEEE American Control Conference (ACC)*, 2013, pp. 4196–4201. 1, 2
- [7] C. Lerch, D. Dong, and I. Abraham, “Safety-critical ergodic exploration in cluttered environments via control barrier functions,” in *IEEE International Conference on Robotics and Automation (ICRA)*, 2023, pp. 10205–10211. 1, 3
- [8] A. Prabhakar, I. Abraham, A. Taylor, M. Schlafly *et al.*, “Ergodic specifications for flexible swarm control: From user commands to persistent adaptation,” in *Conference on Robotics: Science and Systems (RSS)*, 2020, p. 9. 1
- [9] D. Dong, H. Berger, and I. Abraham, “Time optimal ergodic search,” in *Conference on Robotics: Science and Systems (RSS)*, 2023, p. 13. 1, 2, 3
- [10] A. Seewald, C. J. Lerch, M. Chancán, A. M. Dollar *et al.*, “Energy-aware ergodic search: Continuous exploration for multi-agent systems with battery constraints,” in *IEEE International Conference on Robotics and Automation (ICRA)*, 2024, pp. 7048–7054. 1, 3
- [11] K. B. Naveed, D. Agrawal, C. Vermillion, and D. Panagou, “Eclares: Energy-aware clarity-driven ergodic search,” in *IEEE International Conference on Robotics and Automation (ICRA)*, 2024, pp. 14326–14332. 1
- [12] I. Abraham, A. Prabhakar, and T. D. Murphey, “An ergodic measure for active learning from equilibrium,” *IEEE Transactions on Automation Science and Engineering*, vol. 18, no. 3, pp. 917–931, 2021. 1, 3
- [13] Z. Ren, A. K. Srinivasan, B. Vundurthy, I. Abraham *et al.*, “A pareto-optimal local optimization framework for multiobjective ergodic search,” *IEEE Transactions on Robotics*, pp. 1–12, 2023. 1
- [14] A. K. Srinivasan, G. Gutow, Z. Ren, I. Abraham *et al.*, “Multi-agent multi-objective ergodic search using branch and bound,” in *IEEE/RSJ International Conference on Intelligent Robots and Systems (IROS)*, 2023, pp. 844–849. 1
- [15] S. Shetty, J. Silvério, and S. Calinon, “Ergodic exploration using tensor train: Applications in insertion tasks,” *IEEE Transactions on Robotics*, vol. 38, no. 2, pp. 906–921, 2022. 1
- [16] C. Bilaloglu, T. Löw, and S. Calinon, “Whole-body ergodic exploration with a manipulator using diffusion,” *IEEE Robotics and Automation Letters*, vol. 8, no. 12, pp. 8581–8587, 2023. 1
- [17] T. Löw, J. Maceiras, and S. Calinon, “drozBot: Using ergodic control to draw portraits,” *IEEE Robotics and Automation Letters*, vol. 7, no. 4, pp. 11728–11734, 2022. 1
- [18] A. Prabhakar, A. Mavrommatis, J. Schultz, and T. D. Murphey, “Autonomous visual rendering using physical motion,” in *Workshop on the Algorithmic Foundations of Robotics (WAFR)*. Springer, 2020, pp. 80–95. 1
- [19] G. De La Torre, K. Flaßkamp, A. Prabhakar, and T. D. Murphey, “Ergodic exploration with stochastic sensor dynamics,” in *IEEE American Control Conference (ACC)*, 2016, pp. 2971–2976. 1
- [20] E. Ayvalı, H. Salman, and H. Choset, “Ergodic coverage in constrained environments using stochastic trajectory optimization,” in *IEEE/RSJ International Conference on Intelligent Robots and Systems (IROS)*, 2017, pp. 5204–5210. 1
- [21] A. Rao, G. Sartoretti, and H. Choset, “Learning heterogeneous multi-agent allocations for ergodic search,” in *IEEE International Conference on Robotics and Automation (ICRA)*, 2024, pp. 12345–12352. 1
- [22] H. Coffin, I. Abraham, G. Sartoretti, T. Dillstrom *et al.*, “Multi-agent dynamic ergodic search with low-information sensors,” in *IEEE International Conference on Robotics and Automation (ICRA)*, 2022, pp. 11480–11486. 1
- [23] L. Dressel and M. J. Kochenderfer, “On the optimality of ergodic trajectories for information gathering tasks,” in *IEEE American Control Conference (ACC)*, 2018, pp. 1855–1861. 1
- [24] A. Rao, A. Breitfeld, A. Candela, B. Jensen *et al.*, “Multi-objective ergodic search for dynamic information maps,” in *IEEE International Conference on Robotics and Automation (ICRA)*, 2023, pp. 10197–10204. 1
- [25] E. Wittemyer and I. Abraham, “Bi-level image-guided ergodic exploration with applications to planetary rovers,” in *IEEE/RSJ International Conference on Intelligent Robots and Systems (IROS)*, 2023, pp. 10742–10748. 1
- [26] S. Calinon, *Mixture models for the analysis, edition, and synthesis of continuous time series*. Springer, 2020, pp. 39–57. 3
- [27] I. Abraham and T. D. Murphey, “Decentralized ergodic control: Distribution-driven sensing and exploration for multiagent systems,” *IEEE Robotics and Automation Letters*, vol. 3, no. 4, pp. 2987–2994, 2018. 3
- [28] A. Seewald, H. García de Marina, H. S. Midtby, and U. P. Schultz, “Energy-aware planning-scheduling for autonomous aerial robots,” in *IEEE/RSJ International Conference on Intelligent Robots and Systems (IROS)*, 2022, pp. 2946–2953. 4
- [29] A. Wächter and L. T. Biegler, “On the implementation of an interior-point filter line-search algorithm for large-scale nonlinear programming,” *Mathematical Programming*, vol. 106, no. 1, pp. 25–57, 2006. 4
- [30] J. Andersson, J. Åkesson, and M. Diehl, “CasADI: A symbolic package for automatic differentiation and optimal control,” in *Conference on Recent Advances in Algorithmic Differentiation (AD)*. Springer, 2012, pp. 297–307. 4